JOURNAL OF Materials CHEMISTRY

Surface chemical and thermodynamic properties of γ-glycidoxypropyltrimethoxysilane-treated alumina: an XPS and IGC study

Mohamed M. Chehimi,[a] Marie-Laure Abel,[b] John F. Watts*[b] and Roger P. Digby[c]†

[a]*Institut de Topologie et de Dynamique des Systèmes, Université Paris 7 – Denis Diderot, associé au CNRS (UPRESA 7086), 1 rue Guy de la Brosse, 75005 Paris, France*
[b]*School of Mechanical and Materials Engineering, University of Surrey, Guildford, Surrey, UK GU2 7XH*
[c]*Structural Materials Centre, DERA, Farnborough, Hants, UK GU14 0LX*

Received 29th June 2000, Accepted 2nd October 2000
First published as an Advance Article on the web 21st November 2000

Alumina and hydrated alumina were treated with hydrolysed γ-glycidoxypropyltrimethoxysilane (GPS) in aqueous solution. The powder was then dried at various temperatures ranging from room temperature to 120 °C. It was found that the hydration treatment used to create hydroxyl sites was efficient in terms of GPS adsorption. The uptake of GPS was determined by quantitative XPS analysis and the hydrated powders exhibited the highest uptake for all drying temperatures except room temperature. Experiments indicated that it was more favourable to use a hydrated powder that had been dried within the temperature range of 50 to 93 °C to obtain the highest uptake. IGC measurements indicated no variation of the basicity of the specimens examined and little variation of the surface energy. Nevertheless, modification of the acidity was obtained, with the lowest values between 50 and 80 °C drying temperature. Further examination of the C1s XPS signal by peak-fitting of GPS treated powders showed a variation in the type of polar carbons with the treatment temperature. On the basis of the thermodynamic properties and XPS data, two types of interactions between the hydrolysed GPS molecule and the alumina surface are proposed and are correlated with the corresponding temperature. An increase in temperature may lead to opening of the epoxy ring with a subsequent interaction of the silane *via* this side of the molecule. This mechanism occurs jointly with the classical type of interaction expected of silanes *via* the silanol group. It is thought that the former is favoured at high temperature if the GPS film is not damaged. It is also shown that the epoxy functionality is not hydrolysed during hydrolysis of GPS in the aqueous solution.

Introduction

Organosilanes have been used for many years to improve adhesion and the hydrothermal stability of adhesive joints.[1,2] Several approaches have been employed to establish the nature of the interaction occurring at the interface between the silane and the substrate including adsorption isotherms by X-ray photoelectron spectroscopy,[3] composition of the surface by XPS and SIMS,[4,5] or molecular modelling of the silane interaction on the substrate surface.[6] Another approach to the organosilane interaction study on aluminium is to replace the solid metallic substrate by an equivalent to the oxide obtained when oxidised in air. Although the native oxide phase of aluminium is known to be of the γ type,[7] the α type has been chosen in this work, as studies are available by molecular dynamics to assess the interaction of a hydrolysed silane on an α-corundum phase oxide of aluminium.[6]

A factor of interest is the study of one crucial parameter when preparing a substrate for bonding or the formation of an adhesive joint itself: temperature. Although many studies have been performed on joints where organosilanes have been used, very few consider the influence of temperature on the resulting mechanical or interfacial properties. It is the aim of this paper to investigate this aspect of Al_2O_3/GPS bond formation further.

Alumina was treated with a 1% (v/v) aqueous solution of hydrolysed GPS. This is currently used in the aerospace industry for adhesive bonding repairs on aluminium.[8] The effect of drying temperature was subsequently studied as well as the effect of hydration pretreatment. GPS is used in its hydrolysed form where alkoxy groups have reacted with water to form silanols.[5] Prior to GPS adsorption, the Al_2O_3 substrate was treated in pure water to ensure surface hydration. The aim is to create some hydroxyl functionalities which may condense with the silanols of the silane. This is to enhance the interaction of a silane with the oxidised aluminium surface, therefore the adsorption of any silane on the surface. A similar approach was used here to proceed to a pretreatment of the alumina which was therefore treated in water and subsequently dried.

In this work, the surface chemical properties of alumina have been investigated by XPS and the thermodynamic behaviour by inverse gas chromatography (IGC). XPS probes the uptake of GPS and the surface chemistry and IGC the thermodynamic properties of the samples in terms of dispersive interaction and acid–base properties. These two techniques are surface sensitive but it should be noted that XPS probes the whole chemistry of the surface whereas IGC only samples the highest energy sites on the surface.

IGC is now a very well accepted method within the adhesion community as it provides thermodynamic and morphological information on a variety of polymers, fillers and pigments. The term "inverse" means that the stationary phase is under study by contrast to conventional GC in which the mobile phase is of interest. IGC has a well established background for the assessment of γ_s^d, the dispersive contribution to the surface free energy, and acid–base constants. These physicochemical properties are of relevance to adhesion of polymers and

†Current address: GKN Westland Aerospace Ltd., Isle of Wight, UK PO32 6RH.

metal oxides, and can further be used to estimate the reversible work of adhesion at polymer–fibre[9,10] and polymer–pigment[11] interfaces.

The theory and applications of IGC have been reviewed elsewhere.[12–16] IGC has proved effective in the determination of physicochemical properties of several materials as varied as alumina,[17–21] pigments,[11,22] conventional[12,13] and conducting polymers.[23,24]

As far as aluminium and alumina are concerned, Brookman and Sawyer[18] studied salt-modified alumina and showed that these materials selectively separated *cis–trans* isomers and other aromatic hydrocarbons having similar boiling points. The acid–base properties of α-alumina have been found to be strongly dependent on the surface contamination by silica and other metal oxides. For example, Papirer *et al.*[20] showed that 1000 ppm of silica resulted in a significant increase of the acidity of alumina. The controlled surface contamination by various oxides was found to modify the dispersive and acid–base properties of alumina, but more importantly its adsorptive characteristics towards polymers.[21]

Heat treatment of γ-alumina in the presence of water induces structural changes attributed to the formation of a boehmite type compound which lead to an increase of the dispersive component to the surface free energy (γ_s^d) up to 350 °C. This temperature was found to be critical to the transformation of the boehmite back into γ-alumina.[19]

In the case of aluminium oxide trihydrate, γ_s^d as determined by IGC increased sharply from 33.7 to 61.8 mJ m^{-2} (at 47 °C) simply by increasing the drying temperature from 47 to 76 °C. Such modification in the surface thermodynamics of alumina was attributed to water desorption.

Whilst silane-treated fillers (other than alumina) and pigments have frequently been characterised by IGC,[25–29] the latter technique has seldom been applied to silane modification of alumina. Naito *et al.*[30] reported an IGC study of chemically bonded alumina beads prepared with β-phenythyltrichlorosilane. The silane was found to deactivate the beads as judged from the retention data of aliphatic hydrocarbons, benzene and *tert*-butyl methyl ether.

In recent years much of the research performed within our laboratories has been focussed towards studying the specific interactions occurring at interfaces with the help of surface sensitive techniques such as XPS and ToF-SIMS. There is a particular interest in assessing the interactions at the interface between a primer or an adhesive on a metallic surface. Most recent works involve the evaluation of Lewis acid–base interactions between polymers and metallic surfaces,[31] covalent bond formation between silanes and aluminium[32] and silanes interactions with model[33,34] and applied adhesives.[35]

In this paper we compare the physicochemical properties of α-alumina powder before and following hydration and/or GPS treatment. The temperature of cure of the GPS coated alumina was varied between 25 °C and 120 °C. XPS provides a survey of the change in the chemical composition induced by the various treatments and IGC studies were aimed at determining the dispersive and acid–base properties of alumina resulting from the surface treatment.

Experimental

Alumina treatment

12.5 g of alumina powder (Aldrich, 100 μm, α phase) was hydrated in 250 cm^3 of MilliQ water for 30 minutes, then dried at 50 °C for one hour. Then 10 g of this hydrated alumina were treated by 250 cm^3 of a 1% (v/v) aqueous solution of hydrolysed GPS (one hour hydrolysis time), (OSI Silquest) for 30 min. The suspension of alumina in GPS solution was then filtered (without any further solvent rinsing) and left to dry at a temperature ranging from 25 °C to 120 °C.

The GPS-treated hydrated aluminas are abbreviated Al-W-GPS. For cure at *e.g.* 93 °C, the final product will be abbreviated Al-W-GPS93.

For the reference series prepared without water pretreatment, the abbreviation is Al-GPS93 (the number corresponds to the GPS cure temperature). For the reference material hydrated alumina, the abbreviation is Al-W.

X-Ray photoelectron spectroscopy

XPS analyses were carried out using a VG Scientific ESCALAB MkII system operated in the constant analyser energy mode. Mg Kα radiation with an energy of 1253.6 eV was used in all analyses, at a power of 200 W. Although XPS is generally regarded as a non-destructive technique, it has been appreciated for some years that the combination of heat and the high energy component of the Bremsstrahlung radiation from a twin anode source may have a deleterious effect on the sample. To overcome potential problems of sample degradation when using the ESCALAB spectrometer we take the following precautionary measures: the anode is operated at a potential of 10 kV to reduce the Bremsstrahlung component, and the source itself is withdrawn approximately 3 cm to obviate heating effects. This strategy has proved successful for all but the most sensitive of polymeric samples such as poly(vinyl chloride). The samples were mounted on special sample holders that contained the powder and avoided the risk of contamination introduced by other methods such as pressing the powder in indium foil or by preparing pellets. The take-off angle was set at 75°, relative to the horizontal (in the ESCALAB spectrometer, this is horizontal orientation of the sample), to prevent spillage of the powder in the analysis chamber of the spectrometer. Digital acquisition was achieved with a VGS5000 data system based on a DEC PDP11/73 computer, utilising DEC μRSX software, interfaced to the spectrometer. Survey spectra were acquired with a pass energy of 100 eV, and the high resolution spectra with a pass energy of 50 eV. High resolution spectra were recorded for the following elements: C1s, O1s, Al2p, Na1s, Si2p and the Bremsstrahlung induced Si*KLL* transition. A quantitative surface analysis was obtained using the peak areas of the high resolution spectra, following background removal. Wagner sensitivity factors were used for the quantification procedures. Charging of all samples was corrected from the position of neutral carbon contamination at 285 eV.

Quantification of the surface concentration of silicon

For this work, the Auger signal of the silicon was used to quantify the silicon surface concentration. It was not possible to quantify the concentration of silicon from the usual signal Si2p (102 eV) with confidence as there are several secondary signals in this region of the spectrum. First, as the surface concentrations of silicon are low (0.5 to 1.6 at.%) the Si2p signal is perturbed by the sharp slope induced by inelastic electron scattering of Al2p (74 eV) photoelectrons. Additional features can also be detected being induced by secondary X-ray lines from the source such as $MgK\alpha_3$ and $MgK\alpha_4$ (9.2% of the main radiation, 8.4 eV from the source and 5.1% of the main radiation, 10.0 eV from the source respectively) or $MgK\alpha_5$ and $MgK\alpha_6$ (0.8% of the main radiation, 17.3 eV from the source and 0.5% of the main radiation, 20.5 eV from the source respectively).[36] It is therefore more convenient and reliable to use the silicon Auger signal Si*KLL* at higher kinetic energy induced by the Bremsstrahlung component of the X-radiation to quantify the concentration of silicon. Although this feature is rather weak, as it appears in the high kinetic energy region of the spectrum (effectively the negative binding energy region) the background is extremely low. The net effect of this is to yield a spectrum which has surprisingly good signal to noise. In

other work from this laboratory in which we have made use of both the Auger and the photoelectron transitions (*KLL* and 2p) of silicon, the general observation is that the counting statistics of the Auger peak are at least as good as those of the Si2p. The use of this Auger transition was allowable in the current work as all the experiments were performed within a short period of time during which the level of Bremsstrahlung was considered to be constant. For that purpose, an XPS analysis of a pure silica powder (99.9999% Koch-Light Laboratories Ltd.) was performed and the Wagner sensitivity factor of the Si*KLL* transition was deduced from it. It was found to be equal to 0.14 compared to 0.27 for Si2p.

Inverse gas chromatography

A Pye Unicam PU4500 gas chromatograph utilising a flame ionisation detector and a Pye Unicam PU4810 integrator were employed to carry out IGC experiments. Untreated and treated alumina powders were packed in Teflon columns with a diameter of 6.25 mm and length of 45 cm. The ends of the column were plugged with a small amount of clean glass fibre wool.

The carrier gas used was high purity nitrogen, and methane was used as the non-interacting marker. The flow rate was approximately 25 $cm^3\ min^{-1}$ as measured by means of a soap-bubble flowmeter. The column temperature was set at 60 °C, and the injector and detector were held at 100 and 150 °C, respectively. Prior to analysis, the columns were conditioned at 60 °C overnight.

The probes (Table 1) were injected manually with the methane marker by means of a Hamilton gas-tight syringe. The net retention times are calculated by measuring the distance from the non-interacting marker to the centre of the peak of the probe. This procedure was deemed satisfactory because the peaks were symmetrical.

Results and discussion

1. XPS, surface chemical composition of the various alumina powders

Surface concentrations obtained by XPS are given in Table 2 in atomic %.

Effect of washing/hydrating alumina surfaces. Fig. 1 shows the survey spectra of the alumina powder before (a) and after hydration (b). The "as-received" alumina powder clearly exhibits sodium and hydrocarbon contamination along with expected characteristic photoelectron and Auger signals of oxygen (O1s, O*KLL*) and aluminium (Al2p, Al2s). Characteristic peaks arising from sodium (Na1s, Na2s, Na2p) and Na Auger (Na$KL_{23}L_{23}$, NaKL_1L_{23}, NaKL_1L_1) are all present in the survey which is in agreement with the concentration of sodium present (3.3 at.%) at the surface. Neither calcium nor potassium were detected.

The comparison of the survey spectrum of the initial powder with the hydrated/washed alumina shows the disappearance of sodium which has dropped in surface concentration from 3.3 at.% to 0.5 at.%. In the same manner, the carbon concentration has dropped from 16.8 at.% to 9.2 at.%. This range of concentration appears to be fairly small for carbon contamination, this is an effect of the alumina specific surface area. A frequent observation, over many years, from the University of Surrey laboratory, is that clean samples with a high specific area, *e.g.* zeolites and anodized aluminium, exhibit a particularly low surface concentration of carbon. Indeed, when the surface area of a material is high, the carbon signal appears artificially smaller than on a perfectly planar surface. This occurs together with an increase in the oxygen and aluminium surface concentration from 51.0 to 54.7 at.% and 28.9 to 35.5 at.% respectively, generally showing a cleaner surface after hydrating/washing of the alumina.

Table 1 Probes used for IGC measurements

Probe	Abbreviation	Boiling point, bp/°C
n-Pentane	C5	36.1
n-Hexane	C6	69
n-Heptane	C7	98.4
Diethyl ether	DEE	34.6
Chloroform	$CHCl_3$	61.2

Table 2 Surface chemical compositions, in at.%, for all alumina powders

Type of treatment	C	O	Al	Na	Si	Ratio C/Si
Al_2O_3 as received	16.8	51.0	28.9	3.3	[a]	N/A
Al_2O_3-W	9.2	54.7	35.5	0.5	[a]	N/A
Al_2O_3-W-GPS25	10.5	53.2	35.3	0.2	0.9	11.7
Al_2O_3-W-GPS50	8.0	55.5	35.4	0.2	0.9	9.1
Al_2O_3-W-GPS65	9.2	52.0	37.0	0.2	1.6	5.8
Al_2O_3-W-GPS80	9.5	53.2	36.0	0.0	1.3	7.3
Al_2O_3-W-GPS93	5.6	55.4	38.1	0.1	0.7	7.6
Al_2O_3-W-GPS120	4.9	56.7	37.4	0.2	0.8	6.4
Al_2O_3-GPS25	9.2	53.4	35.8	0.7	0.9	10.2
Al_2O_3-GPS50	10.0	54.1	34.7	0.7	0.5	18.5
Al_2O_3-GPS65	11.1	53.5	33.9	0.7	0.9	12.6
Al_2O_3-GPS80	11.6	53.4	33.7	0.5	0.8	15.3
Al_2O_3-GPS93	12.5	52.0	34.4	0.4	0.7	17.6
Al_2O_3-GPS120	6.9	55.9	36.2	0.5	0.6	12.3

[a]Below detection limit.

The first assumption is that the hydration procedure produces hydroxyl (–OH) functionalities at the surface of the alumina and therefore, in addition to the removal of Na_2CO_3 deposit described above, helps the interaction of hydrolysed silane *via* condensation of hydroxyl and silanol. The pure water may also desorbs some impurities at the surface of the alumina and reveal some adsorption sites. This assists the interaction of hydrolysed GPS with alumina.

Hydration of alumina, as shown by XPS, is the object of many discussions in the literature. It is usually agreed that X-ray irradiation as well as loss of energy *via* scattering of the photoelectrons lead to destruction of hydroxyl functionalities at the surface of metal oxides;[37] therefore we did not attempt to demonstrate the creation of hydroxyl functionalities *via* peak-fit of the oxygen signal, although recent work with a monochromated X-ray source has shown this can be done.[37]

Inorganic carbon at the alumina surfaces. Carbon signals have been peak-fitted and are shown in Fig. 2a and b. The as received alumina, shown in Fig. 2a (surface concentration of carbon = 16.8 at.%), exhibits a carbon signal containing both aliphatic hydrocarbon contamination (CC, CH at 285 eV) and polar carbons. The binding energies obtained indicate the presence of carbon carbonyl (287.6 eV), carbonates CO_3^{2-} (289.6 eV), present as an intense signal (a third of all carbon present), in agreement with the literature.[38,39] The fourth component can be assigned to a minor Auger contribution from sodium.[39] After washing/hydration the carbon signal is shown in Fig. 2b (surface concentration of carbon = 9.2 at.%). Only three components are now present which is consistent with sodium removal on the surface of the material. Their binding energies match those mentioned above as seen in Table 3. The concentration of polar carbon is very small either compared to the polar carbon of as received alumina (1.3 at.% as opposed to 8.2 at.% for the as-received alumina) or as a percentage of the surface composition of the hydroxylated alumina. The carbonate surface concentration has dropped and that remaining is very low, less than 1 at.%, attesting to the efficiency of the washing procedure. This indicates that when

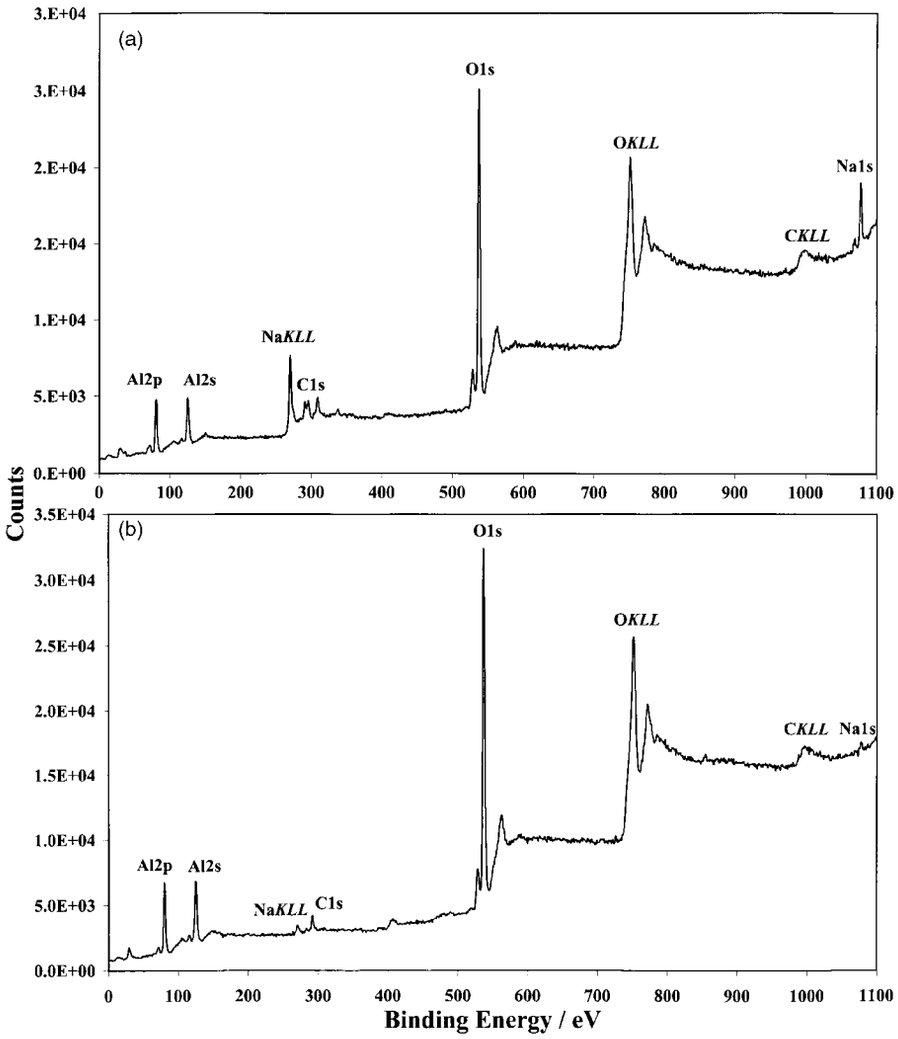

Fig. 1 Survey spectra of alumina (a) as received, (b) after hydroxylation.

using hydrated alumina, the carbonate component will be attenuated as a result of the coating being present. Therefore, the carbon signal of GPS coated hydrated alumina should be an illustration of the carbon functionalities present at the surface as a consequence of the GPS treatment only. This indicates that carbonates will be, at least partly, removed from the alumina surface when treating non-hydrated alumina with GPS aqueous solutions.

The carbonate concentration present in the initial alumina is in a ratio of roughly 1 : 2 compared to sodium (5.5/3.3 = 1.7) which indicates the presence of sodium carbonate. After washing, the concentration of sodium left is very close to the carbonate concentration (0.5 and 0.6 at.% respectively, see Tables 2 and 3). Peak-fitting of the Al2p spectra was also performed but no significant change was noticed either in the binding energy or in the shape of the spectrum.

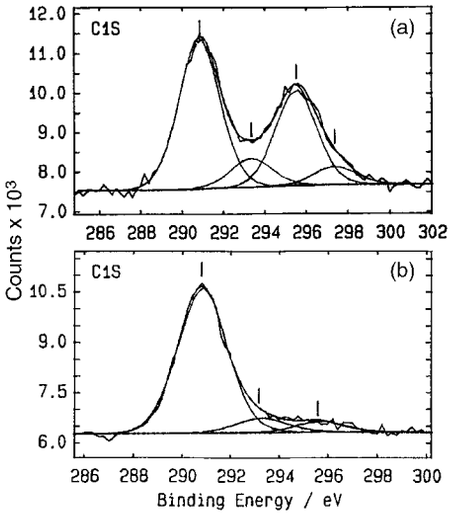

Fig. 2 Carbon C1s peak-fitting of alumina (a) as received, (b) after hydroxylation.

The estimation of silane uptake by XPS. Fig. 3 shows the GPS uptake at all temperatures. It can be seen that in all cases but for one temperature (Al-W-GPS25 and Al-GPS25), the GPS adsorption as detected from the silicon uptake is higher for the powders hydrated in powder prior to GPS adsorption, which is in agreement with the expected effect of the hydration. The two powders dried at room temperature show similar adsorption. The uptake shows a maximum in adsorption for drying temperatures at 65 °C and 80 °C for the hydrated powders when no specific behaviour in adsorption can be observed for the non-hydrated powders. The smallest concentration of silicon is obtained for Al-GPS50, the highest for Al-W-GPS65 and Al-W-GPS80 powders.

Table 2 also indicates the ratio of carbon concentration to silicon concentration. Although the carbon signal will always include a fraction of contamination carbon, the ratio expected

Table 3 Binding energies of carbon from peak-fitting and their respective proportions. Peaks are given in peak-fitting order as the shifts vary slightly. The first peak is always set at 285 eV as it is used for reference

	Peak 1		Peak 2		Peak 3		Peak 4	
Type of treatment	BE	[%]	BE	[%]	BE	[%]	BE	[%]
Al_2O_3 as received	285	8.6	287.6	1.7	289.7	5.5	291.6	1.0
Al_2O_3-W	285	7.8	287.4	0.7	289.8	0.6		
Al_2O_3-W-GPS25	285	7.4	286.9	2.0	289.4	1.1		
Al_2O_3-W-GPS50	285	5.7	286.7	2.1	289.2	0.2		
Al_2O_3-W-GPS65	285	6.0	286.6	2.6	288.8	0.6		
Al_2O_3-W-GPS80	285	6.0	286.6	3.0	288.6	0.6		
Al_2O_3-W-GPS93	285	4.2	286.7	1.1	288.9	0.3		
Al_2O_3-W-GPS120	285	3.8	286.7	0.7	288.9	0.3		
Al_2O_3-GPS25	285	6.5	287.1	1.7	289.5	0.9		
Al_2O_3-GPS50	285	7.2	286.9	2.0	289.5	0.8		
Al_2O_3-GPS65	285	8.1	286.7	2.4	289.4	0.6		
Al_2O_3-GPS80	285	8.1	286.7	2.7	289.5	0.7		
Al_2O_3-GPS93	285	9.5	286.9	2.4	289.8	0.6		
Al_2O_3-GPS120	285	5.2	286.8	1.5	289.2	0.3		

for GPS is equal to six. It can clearly be seen that carbon is present in a higher concentration than expected for all non-hydrated powders and also for the hydrated powders dried at 25 °C and 50 °C.

Peak-fitting of the carbon 1s spectrum of the treated powders. Peak-fitting of the carbon allows the determination of the proportion of aliphatic, unfunctionalised carbon to polar carbon. The polar carbon contribution is clearly made up of two components at separations of *ca.* 1.6 eV and 3.6 eV from the main, unfunctionalised carbon peak. The exact position of the component is found to be a function of the sample history, and an initial view of the nature of the carbonaceous material may be gained by grouping these two contributions together. All peak-fitting data are reported in Table 3, together with the respective surface concentrations of neutral and polar carbon. Fig. 4 shows an example of carbon peak-fitting, in this case hydrated alumina dried at 80 °C after GPS adsorption, Al-W-GPS80.

The GPS molecule contains four carbons attached to oxygen against two aliphatic carbons of CC, CH type. The ratio of neutral carbon to polar carbon is equal to 2 for the hydrolysed GPS structure. Therefore, one way to assess GPS adsorption and retention on the alumina surface from the carbon signal is to examine the concentration of polar carbons. However, polar carbon may also be present on the surface as a result of adventitious contamination. Therefore, to check whether this approach is valid for this work, we plotted the concentration of silicon in atomic percentage *versus* the true concentration of polar carbons (Fig. 5). In the case of hydrated alumina, the correlation is good (correlation coefficient > 0.75), but for the as-received alumina (not shown here) the agreement is very poor (correlation coefficient = 0.46). This means that any change in the polar carbon concentration for hydrated powders subsequent to adsorption occurs as a result of GPS adsorption. Unfortunately, this also means that carbon data from the non-hydrated powders are not so reliable as the silicon uptake data. This is probably due to the fact that carbon contamination, such as carbonate, was not as well removed from the surface compared to a washed, hydrated alumina. This is also illustrated in Fig. 6a and b, where the surface concentration of each type of carbon has been plotted according to the treatment of powders. For neutral carbons, shown in Fig. 6a, the pretreated alumina shows a trend towards the decrease from hydrated (only) powder to Al-W-GPS120. When the alumina is not hydrated there is mainly an increase in the

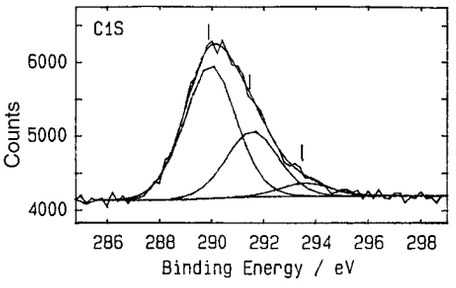

Fig. 4 Example of carbon C1s peak-fitting for coated powders: Al-W-GPS80.

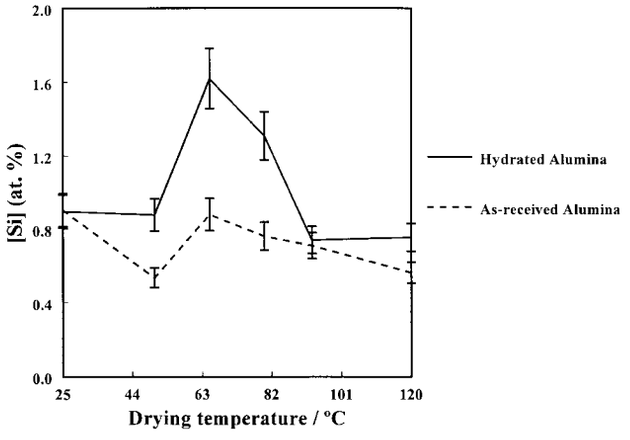

Fig. 3 Plots of the silicon surface concentration *vs.* temperature for both types of specimens.

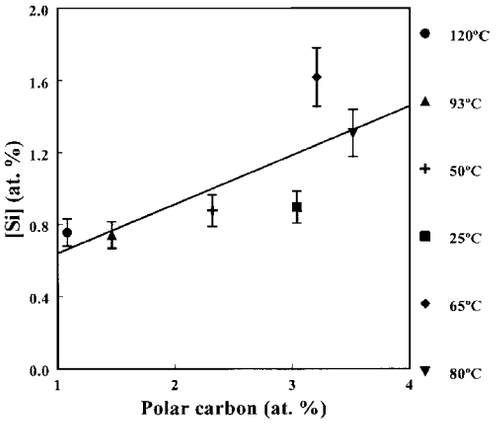

Fig. 5 Correlation of silicon surface concentration *vs.* surface concentration of polar carbons for hydrated alumina.

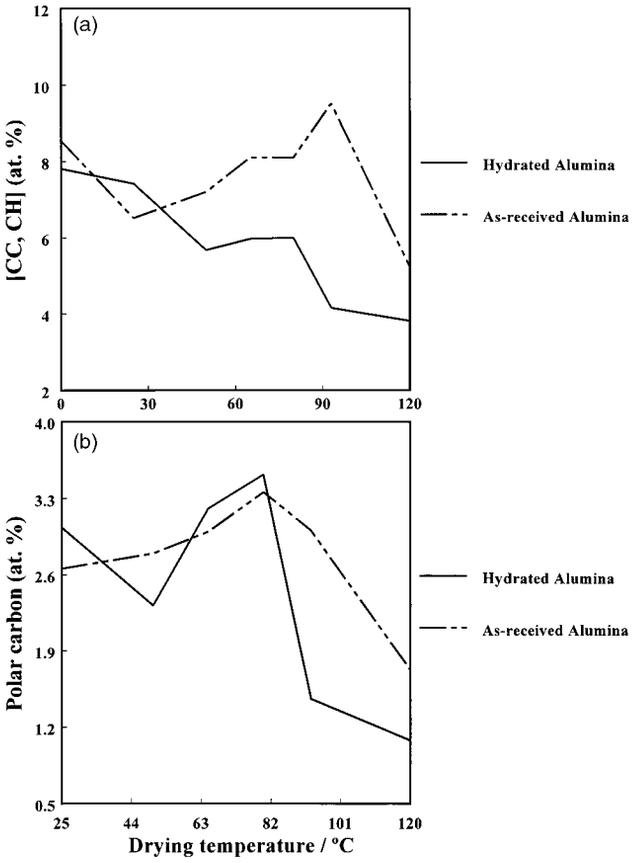

Fig. 6 Surface concentration of: (a) neutral carbons, (b) polar carbons, *vs.* temperature for both types of specimens.

concentration followed by a decrease (Fig. 6a) with a maximum at 93 °C. The concentration of the polar carbons in Fig. 6b increases then decreases with a maximum for the non-hydrated powders at Al-GPS80. Two maxima are obtained for hydrated powders: Al-W-GPS65 and Al-W-GPS80. This is in line with the correlation described above, *i.e.* the respective maximum concentration of silicon and carbon being obtained from the same two samples.

Another approach to these data is to discuss them in terms of shifts of the polar carbons according to the temperature of drying. The peak-fitting of the carbon signal was obtained and the chemical shifts displayed as a function of the drying temperature. This is shown for the first polar carbon in Fig. 7 together with some characteristic shifts obtained from

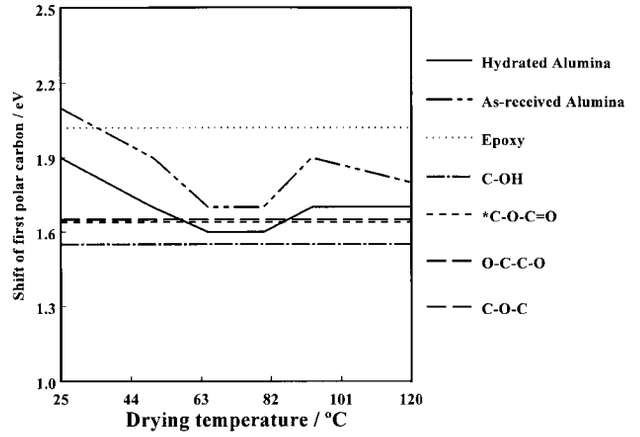

Fig. 7 Shift of first polar carbon *vs.* temperature for both types of specimens.

the literature for various polar carbons. A secondary shift has been taken into account for the carbons of the C–O–C type because of the vicinity of the epoxy ring. The variation of the shifts in the case of both hydrated and non-hydrated alumina shows a similar trend although with always higher shifts in the case of the non-primarily hydrated samples. As mentioned before, hydrolysed GPS has several polar carbons in the structure but according to the temperature the chemical shift changes. Al-W-25, Al-GPS25 and Al-GPS50 exhibit a shift close to an epoxy functionality which indicates a protection of the functionality during the hydrolysis and deposition process. As for other polar carbons, the ether type is expected from GPS, this may also indicate a preferential orientation of the epoxy towards the surface. Seven of the samples: Al-W-GPS50, Al-GPS65, Al-W-GPS65, Al-GPS80, Al-W-GPS80, Al-W-GPS93 and Al-W-GPS120, exhibit a shift for the first polar carbon that can be assigned to either *C–O–C=O, C–O–C or C–OH functionalities. It is less clear whether the Al-GPS93 and Al-GPS120 shifts can be assigned to epoxy or *C–O–C=O/C–OH/C–O–C. Taking into account the expected type of carbon functionalities consequent to either contamination or GPS adsorption, the former is very unlikely. The chemical shifts of the second polar carbon were not plotted as a function of temperature as they are mostly assigned to carbonates.

2. Surface thermodynamic properties by means of IGC

Theory of thermodynamics by IGC. IGC is based on the interfacial interactions between molecular probes and the stationary phase. Probes are injected at infinite dilution so that lateral probe–probe interactions are negligible and the retention is governed by solid–probe interactions only.

The volume of carrier gas required to sweep out an adsorbed species is the net retention volume, V_N:

$$V_N = jF_C t_N \quad (1)$$

where j is the compression factor, F_C the corrected flow rate and t_N the net retention time. The value of V_N will therefore be large for a strongly adsorbed species.

At infinite dilution (zero coverage), ΔG_a, the free energy of adsorption, is related to V_N by:

$$-\Delta G_a = RT \ln V_N + C \quad (2)$$

where R is the gas constant and T the working temperature. C is a term that takes the weight and specific surface area of the stationary phase, and the standard state of the probes in the gaseous and adsorbed state into account.[40] Combining eqn. (1) and (2), one obtains the following relationship:

$$-\Delta G_a = RT \ln t_N + C' \quad (3)$$

The determination of ΔG_a or $RT\ln t_N$ values for all material–probe pairs will permit us to assess γ_s^d and acid–base constants for the materials under test. γ_s^d and acid–base constants will be assessed using n-alkanes and specific probes, respectively.

Fig. 8 shows chromatograms of all probes and methane injected in columns packed with Al-W and Al-W-GPS50. The increasing trend of net retention time for probes adsorbed onto Al-W (Fig. 8a) is:

$$C5 < C6 < C7 < CHCl_3 < DEE$$

This trend is the same as that found for untreated alumina. In the case of Al-W-GPS50 (Fig. 8b), there is a dramatic change in the chloroform–DEE sequence and the new increasing trend of net retention times is:

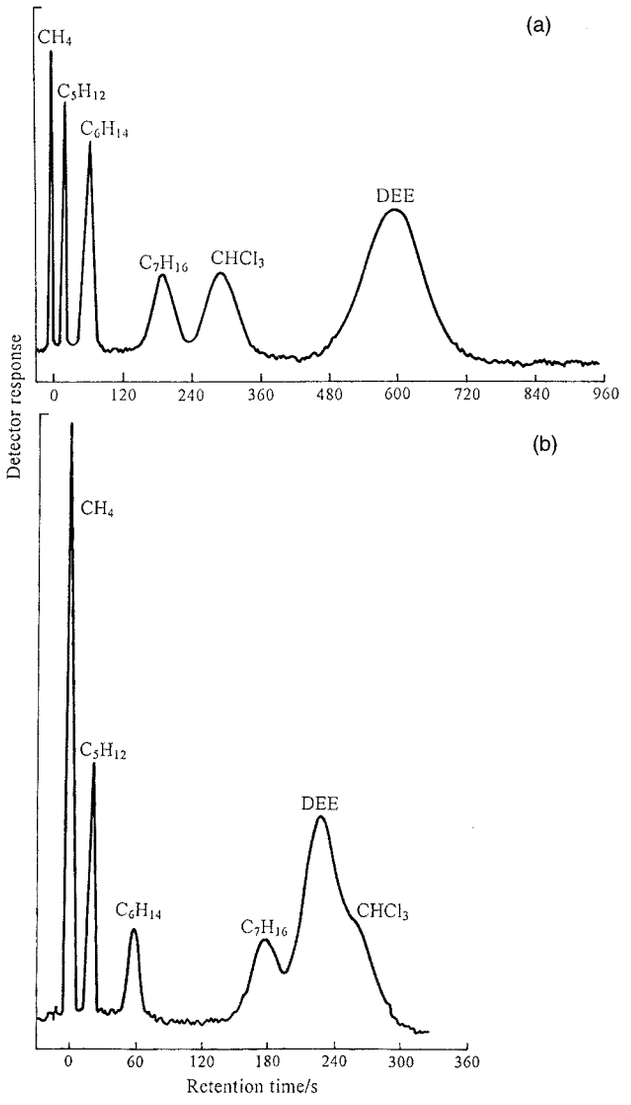

Fig. 8 Chromatograms of all probes and methane for (a) Al-W and (b) Al-W-GPS50.

$$C5 < C6 < C7 < DEE < CHCl_3$$

There is thus clear evidence for the modification of the acid–base properties of hydrated alumina as a result of GPS treatment. This will be shown quantitatively below.

For all the alumina–probe pairs characterised in this work, t_N values (in seconds) are reported in Table 4.

$RT\ln t_N$ values (not shown here) were plotted *versus* the number of carbon atoms per n-alkane for the homologous series of n-alkanes adsorbed onto the untreated alumina, Al-W, Al-W-GPS50 and Al-W-GPS93. Excellent linear correlation was generated by the n-alkane probe molecules. The gradient of each plot is a measure of ΔG_a^{CH2}, the free energy of adsorption per methylene group, the square of which is proportional to γ_s^{d}.[41] The values obtained, as indicated in Table 5, show very comparable gradients (3 ± 0.1 kJ mol^{-1}) for untreated and treated aluminas. Therefore, neither water nor GPS significantly affected the dispersive properties of the various alumina samples under test.

If the material under test and a molecular probe interact *via* both dispersive and acid–base forces, it is assumed that ΔG_a has two additive dispersive (d) and acid–base (AB) contributions:

$$\Delta G_a = \Delta G_a^{\,d} + \Delta G_a^{\,AB} \quad (4)$$

There are a number of methods to assess the contribution of ΔG_a^{AB} to ΔG_a of a material.[9,18,42–48] A simple approach uses the boiling points of the probe molecules. If the ΔG_a values of the n-alkanes are plotted against their boiling points a straight line should be attained. Then if specific acid–base interactions occur between a probe molecule and the stationary phase, ΔG_a value of the specific probe will deviate from the reference line due to the n-alkanes. Combining eqn. (3) and (4), ΔG_a^{AB} can be computed by:

$$-\Delta G_a^{\,AB} = -\left(\Delta G_a - \Delta G_a^{\,d}\right) = RT\ln(t_N/t_{N,ref}) \quad (5)$$

where t_N and $t_{N,ref}$ are the net retention times of the polar probe and a hypothetical reference n-alkane having the same boiling point, respectively.

In this work we have used DEE and chloroform as the reference Lewis base and acid, respectively. The rationale for using a combination of these two probes is that they have a very low degree of self-association[49] so that they behave as a pure base and a pure acid, respectively. In the terminology of Berg,[50] they would be called "monofunctional" specific probes. In their study of various alumina surfaces, Papirer *et al.*[21] used a combination of DEE and dichloromethane to monitor the acid–base characteristics of the materials. We preferred to use chloroform rather than dichloromethane as the latter dimerizes in inert liquids[51] and may interact with solid surfaces[52] *via* double hydrogen bonding.

Fig. 9 shows a graph of $RT\ln t_N$ values plotted against the boiling point of the probe molecules for Al-W-GPS93. Again the n-alkanes yield a straight line. The distance between the specific probe markers and the reference line is a measure of ΔG_a^{AB}, the acid–base contribution to the free energy of adsorption. For either the untreated or treated alumina, the markers corresponding to DEE and chloroform are invariably lying off the dispersive interactions reference line, an indication

Table 4 Net retention times (s) for n-alkanes and specific probes adsorbed onto untreated and treated alumina powders at 60 °C

Probe	Al	Al-GPS25	Al-GPS50	Al-GPS65	Al-GPS80	Al-GPS93	Al-GPS120
C5	31.4	41.4	21.9	21.3	19.3	29.6	22.8
C6	92.6	127.1	65.9	67.5	58.6	85.4	71.3
C7	269.2	387.9	199.2	208.2	177.2	251.6	217.6
DEE	972.6	793.8	401.4	404	240	431.4	443
$CHCl_3$	465.5	564.6	309.9	317.8	282	385.2	336.2
Probe	Al-W	Al-W-GPS25	Al-W-GPS50	Al-W-GPS65	Al-W-GPS80	Al-W-GPS93	Al-W-GPS120
C5	22.6	23.7	21.1	22.4	20.5	25.2	28.3
C6	65.7	72.5	60	66.4	60.5	76.1	87.3
C7	194.6	227.5	176.2	202.8	180.8	231.8	266.4
DEE	591.7	510.3	222.1	280.4	242.2	491.2	582.3
$CHCl_3$	294.8	322.8	256.8	291	257.6	330.9	380.6

Table 5 γ_s^d (mJ m^{-2}) values and α (acidity)[a] and β (basicity)[a] constants determined for untreated and treated alumina samples at 60 °C

	$-\Delta G_a^{CH2}$	γ_s^d	α	β	t_N(DEE)/t_N(C5)	t_N(CHCl$_3$)/t_N(C6)
Al_2O_3	2.974	50.8	9.694	5.116	30.9	5.02
Al-GPS25	3.099	55.2	8.382	4.794	19.2	4.44
Al-GPS50	3.058	53.7	8.258	4.931	18.3	4.70
Al-GPS65	3.157	57.3	8.346	4.986	19.0	4.71
Al-GPS80	3.073	54.2	7.185	5.009	12.5	4.81
Al-GPS93	2.966	50.5	7.631	4.787	14.6	4.51
Al-GPS120	3.124	56.1	8.413	4.984	19.4	4.72
Al-W	2.981	51.1	9.247	4.774	26.2	4.49
Al-W-GPS25	3.132	56.4	8.721	4.782	21.5	4.46
Al-W-GPS50	2.936	49.5	6.724	4.623	10.5	4.28
Al-W-GPS65	3.054	53.6	7.220	4.719	12.5	4.39
Al-W-GPS80	3.015	52.2	7.044	4.643	11.8	4.26
Al-W-GPS93	3.054	53.6	8.430	4.714	19.5	4.35
Al-W-GPS120	3.104	55.3	8.559	4.722	20.6	4.36

[a] $\alpha = -\Delta G_a^{AB}$(DEE), and $\beta = -\Delta G_a^{AB}$(CHCl$_3$).

of strong specific interactions with the solid surface.

The properties of the solid materials, namely γ_s^d and acid–base constants, are derived from the raw data reported in Table 4.

γ_s^d is proportional to the square of ΔG^{CH2}:[41]

$$\gamma_s^d = (1/4\gamma_{CH2})\left(\Delta G^{CH2}/Na_{CH2}\right)^2 \quad (6)$$

where N is the Avogadro number, a_{CH2} is the cross-sectional area of an adsorbed CH_2 group (6 Å^2), γ_{CH2} is the surface free energy of a solid containing only methylene groups such as polyethylene ($\gamma_{CH2} = 36.8 - 0.058T$(°C)).

We define α and β parameters as acidity and basicity constants of the solid materials as follows:

$$\alpha_{DEE} = -\Delta G_a^{AB}(DEE) \quad (7)$$

and

$$\beta_{CHCl3} = -\Delta G_a^{AB}(CHCl_3) \quad (8)$$

α_{DEE} and β_{CHCl3} values are derived from the values in Table 4 and plots similar to those shown in Fig. 9.

Acid–base and dispersive properties by means of IGC. The results reported in Table 5 show quantitatively that untreated and treated alumina samples have medium values of γ_s^d in the narrow 49.5–57.3 mJ m^{-2} range. These values appear thus to be almost independent of water and/or GPS treatments. For the untreated alumina, γ_s^d is relatively lower than the values reported by Papirer *et al.*[21] at 60 °C. This is perhaps due to surface contamination and low conditioning temperature (60 °C). The values reported in Table 5 are rather comparable with those of aluminium oxide trihydrate.[17]

The acid–base properties reported in Table 5 show that DEE strongly interacts with alumina samples (α values), and that this acid–base interaction is 1.5 to 2 times stronger than the acid–base interaction of chloroform. However, there is not much to be gained from the values of β since they only vary slightly upon alumina treatment with water. β values remain almost independent of the cure temperature of GPS. Actually, only the DEE solute is able to probe the subtle changes at the alumina surface induced by either water and/or GPS pretreatment.

In Fig. 10 we have plotted the DEE/C5 net retention time ratio for the various Al-W-GPS and Al-GPS materials and their corresponding reference materials alumina and Al-W. t_N(DEE)/t_N(C5) matches the ($t_N/t_{N,ref}$) for DEE determined by eqn. (5), since DEE and C5 have comparable boiling points. Using the t_N(DEE)/t_N(C5) ratio might be more appropriate than α values since the variations of the retention time ratio are not lost in the logarithmic scale. Whilst α values change by 2–3 kJ mol^{-1} and thus not more than 30% of the value reported for untreated alumina, the t_N(DEE)/t_N(C5) ratio changes three fold.

In the case of the Al-W-GPS series, Fig. 10 shows clearly that water pretreatment affects the surface of alumina and that GPS brings about additional changes in the chemical structure of the adsorbed or grafted overlayer. Acidity decreases to get to the lowest t_N(DEE)/t_N(C5) ratios obtained over the range of GPS cure temperatures between 50 °C and 80 °C. Finally, there is again a jump of the acidity of the surface for a cure temperature of 93 °C as measured by the t_N(DEE)/t_N(C5) ratio. This seems indeed to be a critical temperature of GPS cure as no more significant change is observed for the GPS cure at 120 °C.

In the case of the Al-GPS series, there is evidence for grafting or adsorbing GPS. However, this series behaves in a different manner than Al-W-GPS as a function of cure temperature.

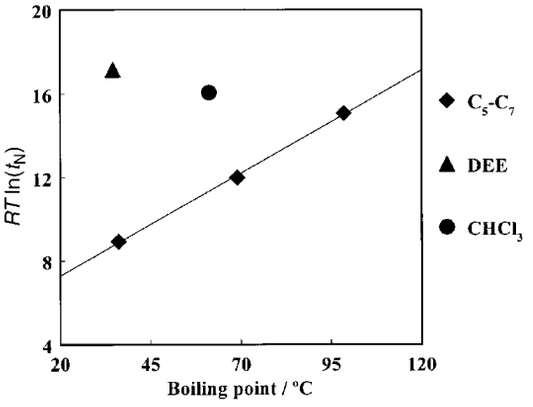

Fig. 9 Plot of $RT\ln t_N$ *vs.* the boiling point T_b of all probes for Al-W-GPS93.

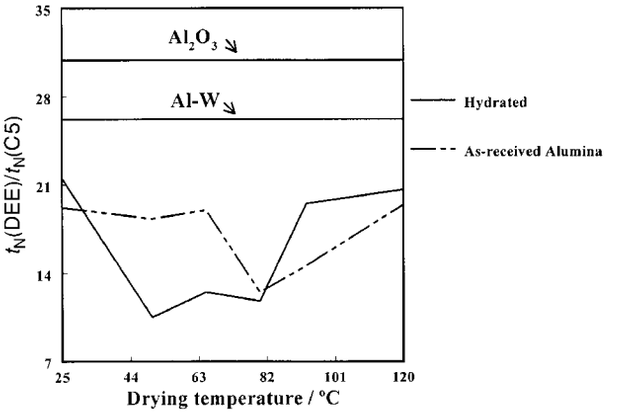

Fig. 10 Plot of the DEE/C5 net retention times for the various specimens *vs.* temperature.

Still, 80 °C is again an onset temperature of cure whereas 93 °C is no longer a critical temperature of GPS cure. Fig. 10 indicates that for the Al-GPS series there is possibly a degree of hydration of alumina followed by adsorption of GPS. However, this hydration is most probably not as effective as that of the Al-W-GPS series.

3. Effect of the temperature on GPS coating

There are very few studies concerning the degradation of organosilane coupling agents. In most applications, it is assumed that the silane is fulfilling its role as adhesion promoter without considering the effect that the various process parameters have on its performance and chemistry, particularly temperature. We believe that high temperatures affect the chemical nature of the silane grafted to the substrate, which may be degraded when the temperature increases above a certain threshold. For its use in any adhesion process, it is highly desirable to understand the effect of temperature on the interaction of the GPS silane with alumina and on the surface thermodynamic properties.

Dispersive properties. The IGC results indicate that neither water nor GPS significantly affected the dispersive properties of the various alumina samples under test. One possible explanation of the low variation of γ_s^d values is the presence of carbon contamination. Indeed, although the actual concentration of neutral carbon varies from 3.9 to 7.4 at.% for the treated specimens, its proportion of the carbon signal is always very high and above 60% of the total carbon signal. The two types of powders dried at the highest temperature, 120 °C, exhibit the smallest actual concentration of neutral carbon and also some of the highest surface free energies (56.1 and 55.3 mJ m^{-2} for the non-treated and pretreated powder respectively). There does not, however, seem to be any direct correlation between the proportion of neutral carbon on the surface and the dispersive properties. Other dispersive contributions have to be taken into account from other functionalities.

Acid–base properties. *Al_2O_3 and hydrated Al_2O_3.* Unexpectedly the acid–base properties did not vary much before and after the hydration process. It was found that both acidity and basicity decreased. This is probably due to the disappearance of sodium (acid) and carbonate (basic) ions, despite the fact that hydrating the surface creates acidic hydroxyl sites.

Acid–base properties for GPS coated powders. As shown above, the correlation between the concentration of polar carbons and the concentration of silicon is reasonably high in the case of pretreated powders. For a good correlation, the polar carbon chemical shift is a direct illustration of the bond type between GPS and alumina and carbon functionalities present at the surface of alumina. Hence, this allows a discussion on the effect of drying temperature on the basis of the polar carbon chemical shifts. Fig. 3 indicates an increase in silicon concentration from 50 °C to 80 °C followed by a drop with low levels of GPS at 93 °C and 120 °C. This may indicate either a degradation of the GPS molecule above 80 °C or may be a reorientation of the molecule. This is a possibility as the concentrations of silicon obtained are small, between 0.54 and 1.6 at.%, and therefore such a phenomenon will have more impact on the results obtained. Of the two possibilities the former is more plausible. Bertelsen and Boerio have shown that drying a GPS film on aluminium at temperatures higher than 180 °C degrades the molecules by opening of the epoxy ring and leads to formation of carbonyl functionalities.[53,54] If degradation occurs, this shows that only a window between 65 °C and 93 °C is favourable for the interaction of GPS with the alumina surface. Although the same correlation could not be established for the non-treated powders, the same drop is observed after 80 °C.

As indicated by the epoxy functionality reactivity in the presence of water, there is a clear possibility of ring opening from the conditions used during the hydrolysis step (and also when the hydrolysed GPS is put in the presence of the hydroxylated surface). When GPS is in solution to be hydrolysed, there is some evidence that the epoxy functionality is protected by the silanol groups.[53,55] This is somehow confirmed by the binding energy of the first polar carbon for Al-W-GPS25, Al-GPS25 and Al-GPS50, samples for which the shift is the closest to a carbon epoxy. It should be noted also that their surface thermodynamic properties are very similar.

For the majority of the specimens, the assignment of the first polar carbon has been assigned to C–O–C, C–OH or *C–O–C=O functionalities. It is thought that the temperature can not affect the bonding of the different species in such a way that we obtain the latter. In comparison, the second functionality can easily be obtained by opening of the ring to interact with a hydroxyl bound to aluminium, although the binding energy of the first polar carbon is probably a combination of the two. C–O–C is obtained simply as a result of the GPS adsorption, as two of the carbons neighbour an oxygen in the initial molecule. The examination of the acid–base properties shows that there is a decrease then an increase of the acidity. The condensation of silanols from GPS and hydroxyls, and also silanols between them, may result in a decrease of the acidity of the surface *via* disappearance of acidic hydroxyl sites/functionalities. This is indeed obtained between 50 °C and 80 °C for the pretreated powders and for Al-GPS80 as shown in Fig. 10. Surprisingly, instead of reaching a steady state for which the acidity of the surface would be constant, we see it increase again above 80 °C in all cases. The thickness of a GPS film is expected to decrease with temperature,[34,56] as a result of crosslinking, dehydration or degradation; therefore for a very thin coverage, the alumina surface may be partially undercovered. This may lead to an increase of the acidity as a consequence, for the alumina, either in its as-received or hydrated form, is more acidic than any of

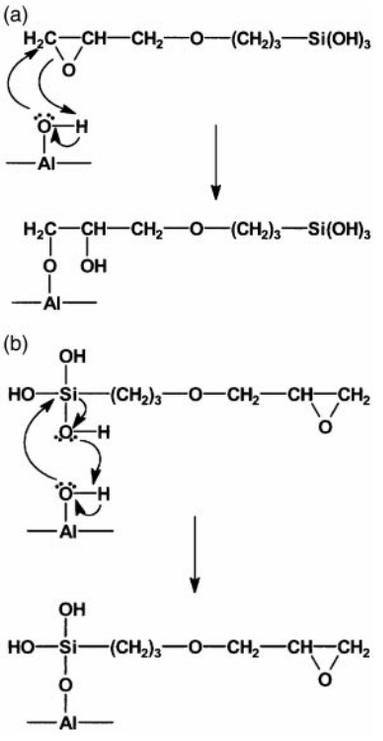

Fig. 11 Possible interactions between hydrolysed GPS and alumina: (a) interaction *via* epoxy ring; (b) interaction *via* silanol.

the treated powders. The increase of the surface acidity may be explained by a different kind of interaction. Fig. 11 shows the possible interactions between alumina and hydrolysed GPS. The first reaction (Fig. 11a) illustrates the opening of the epoxy ring resulting in the creation of alcohol functionalities in agreement with the chemical shift obtained by XPS. Note that this reaction leads to the creation of an organic acidic site. This alcohol would replace the hydroxyl lost on the alumina surface and would then give rise to the acidity again. This type of interaction assumes that part of the hydrolysed GPS molecules will at least lie down flat on the alumina surface to interact on both sides of the molecule. This was indeed observed using molecular modelling of GPS interactions on a model surface of corundum, *i.e.*, amorphous α type of alumina.[6] The second reaction (Fig. 11b) shows the interaction of the silanol side of GPS with the alumina. This reaction is probably enhanced by the increase of temperature especially approaching 100 °C as the water is more likely to evaporate when reaching its boiling point, but the mechanism showing the opening of the epoxy ring is also favoured by increasing the temperature as indicated by the polar carbon binding energy shift. The possibility of further reactions has been examined and on the basis of the IGC results, which indicate an increase of acidity in the temperature range of 80–120 °C, it is proposed that only the organofunctional end of the GPS molecule interacts with the alumina substrate at these temperatures. The trisilanol end remains unattached and the epoxy ring opened which accounts for the change in acid–base properties. The lack of a formed bond is in contrast to previous high resolution ToF-SIMS work on aluminium substrates.[32]

The acid–base properties of the surface are probably a result of the combination of the two reactions (a and b in Fig. 11), the former being more apparent above 80 °C. There is a possibility that the temperature increase above 80 °C leads to the destruction of hydroxyl sites on the alumina surface or to dehydration of the surface by increase of temperature (loss of H_2O) which may induce a reaction with the epoxy as less hydroxyl sites are available.

We believe this effect is less obvious for the non-hydrated powders as less interaction sites are available and as the polar carbons are exhibiting a binding energy intermediate between an epoxy and an alcohol or ether type of carbon. The nature of the aluminium oxide present at the outer surface of an aluminium substrate varies with temperature and may be an important factor as the type of interaction when a silane coating is deposited. More particularly, in the case of pure aluminium a transition in the type of oxide is observed at 75 °C from $Al_2O_3{\cdot}3H_2O$ to $Al_2O_3{\cdot}H_2O$ or boehmite.

Conclusions

In this paper, we examined GPS treated alumina by both XPS and IGC to determine the surface chemistry and thermodynamic properties.

1. It was found that the washing/hydration procedure was effective in terms of increasing GPS adsorption.

2. In terms of thermodynamic properties it was shown that there is very little variation according to the type of treatment and temperature of drying concerning the dispersive properties. There is no obvious correlation between them and the neutral carbon contamination on the surface either. No variation of the basicity of the surface was obtained.

There is, nevertheless, an influence of the hydration pretreatment and temperature of drying on the type of functionality present at the surface of the specimens and also on the acid–base properties. This is observed as a decrease of the surface acidity between 50 and 80 °C then an increase above 80 °C. The decrease may be partly explained by the "classic" interaction described below and the decrease by partial undercovering of the alumina surface as a consequence of poor coverage.

3. Two interactions have been proposed and this behaviour is more obvious for the hydrated powders: a "classic" interaction of the silanol side with hydroxyl on the alumina surface or interaction of the epoxy ring with hydroxyls at the surface of the alumina resulting in the opening of the epoxy with formation of an alcohol type of functionality. The results indicate that the latter reaction is favoured at the higher temperatures used in this work if the GPS is not damaged at too high temperature.

Acknowledgements

MMC thanks the University of Surrey Research Promotion Initiative Scheme. The authors thank Professor J. N. Hay for the use of the IGC equipment and have very much appreciated the technical assistance of Mr V. Zettel with IGC measurements, and Mr S. Greaves for the XPS measurements. Fig. 8a and b by Sheila Rudman.

References

1 E. P. Pluedemann, in *Silane Coupling Agents*, Plenum Press, New York, 1991.
2 *Silanes and Other Coupling Agents*, ed. K. L. Mittal, VSP, Utrecht, 1992.
3 R. Bailey and J. E. Castle, *J. Mater. Chem. Sci.*, 1977, **12**, 2049.
4 S. J. Davis and J. F. Watts, *Int. J. Adhes. Adhes.*, 1996, **16**, 5.
5 M-L. Abel, J. F. Watts and R. P. Digby, *Int. J. Adhes. Adhes.*, 1998, **18**, 179.
6 P. M. Hobbs and A. J. Kinloch, *J. Adhes.*, 1998, **66**, 203.
7 C. R. Werrett, D. R. Spyke and A. K. Bhattachiarya, *Surf. Interface Anal.*, 1997, **25**, 809.
8 R. P. Digby and S. J. Shaw, *Int. J. Adhes. Adhes.*, 1998, **18**, 261.
9 J. Schultz, L. Lavielle and C. Martin, *J. Adhes.*, 1987, **23**, 45.
10 M. Nardin, E. M. Asloun and J. Schultz, *Surf. Interface Anal.*, 1991, **17**, 485.
11 J. Lara and H. P. Schreiber, *J. Coat. Technol.*, 1991, **63**, 81.
12 *Inverse Gas Chromatography. Characterization of Polymers and Other Materials*, ed. D. R. Lloyd, T. C. Ward and H. P. Schreiber, ACS Symposium Series No 391, American Chemical Society, Washington DC, 1989.
13 Z. Al-Saigh, *Polym. News*, 1994, **19**, 269.
14 P. Mukhopadhyay and H. P. Schreiber, *Colloids Surf. A*, 1995, **100**, 47.
15 E. Papirer and E. Brendlé, *J. Chim. Phys.*, 1998, **95**, 122.
16 M. M. Chehimi, in *Adhesion Promotion Techniques for Advanced Technologies*, ed. K. L. Mittal and A. Pizzi, Marcel Dekker, New York, 1999, ch. 2, p. 27.
17 H. Balard and E. Papirer, *Prog. Org. Coat.*, 1993, **22**, 1.
18 D. J. Brookman and D. T. Sawyer, *Anal. Chem.*, 1968, **40**, 106.
19 E. Papirer, G. Ligner, A. Vidal, H. Balard and F. Mauss, in *Chemically Modified Oxide Surfaces*, ed. E. Leyden and W. T. Collins, Gordon and Breach, New York, 1990, p. 361.
20 E. Papirer, J. M. Perrin, B. Siffert and G. Phillipponeau, *J. Phys. (Paris)*, 1991, **III**, 697.
21 E. Papirer, J. M. Perrin, B. Siffert and G. Phillipponeau, *J. Colloid Interface Sci.*, 1991, **144**, 263.
22 H. P. Schreiber and F. St Germain, in *Acid–Base Interactions: Relevance to Adhesion Science and Technology*, ed. K. L. Mittal and H. R. Anderson Jr., VSP, Utrecht, 1991, p. 273.
23 M. M. Chehimi, M-L. Abel and Z. Sahraoui, *J. Adhes. Sci. Technol.*, 1996, **10**, 287.
24 M. M. Chehimi, M.-L. Abel, C. Perruchot, M. Delamar, S. F. Lascelles and S. P. Armes, *Synth. Met.*, 1999, **104**, 51.
25 A. C. Tiburcio and J. A. Manson, *J. Appl. Polym. Sci.*, 1991, **42**, 427.
26 A. K. Bledzki, J. Lieser, G. Wacker and H. Frenzel, *Composite Interfaces*, 1997, **5**, 41.
27 P. H. Harding and J. C. Berg, *J. Adhes. Sci. Technol.*, 1997, **11**, 471.
28 J. M. Felix, P. Gatenholm and H. P. Schreiber, *Polym. Composites*, 1993, **14**, 449.
29 M. J. Wang and S. Wolff, *Rubber Chem. Technol.*, 1992, **65**, 715.
30 K. Naito, K. Kudo and S. Takei, *Anal. Sci.*, 1992, **8**, 169.
31 S. R. Leadley and J. F. Watts, *J. Adhes.*, 1997, **60**, 175.

32 M-L. Abel, R. P. Digby, I. Fletcher and J. F. Watts, *Surf. Interface Anal.*, 2000, **29**, 115.
33 M-L. Abel, A. Rattana and J. F. Watts, *Langmuir*, 2000, **16**, 6510.
34 A. Rattana, MSc thesis dissertation, University of Surrey, 1999.
35 J. Hermes, A. Rattana, M-L. Abel and J. F. Watts, *Surf. Interface Anal.*, to be submitted.
36 *Practical Surface Analysis, Volume 1: Auger and X-ray Photoelectron Spectroscopy*, ed. D. Briggs and M. P. Seah, John Wiley and Sons, Chichester, 1990.
37 M. R. Alexander, G. E. Thompson and G. Beamson, *Surf. Interface Anal.*, 2000, **29**, 468.
38 *High Resolution XPS of Organic Polymers. The Scienta ESCA300 Database*, G. Beamson and D. Briggs, John Wiley and Sons, Chichester, 1992.
39 *Handbook of X-ray Photoelectron Spectroscopy*, ed. J. Chastain and R. C. King, Phy Elec. Inc., Eden Prairie, MN, USA, 1995.
40 E. F. Meyer, *J. Chem. Edu.*, 1980, **57**, 120.
41 G. M. Dorris and D. G. Gray, *J. Colloid Interface Sci.*, 1980, **77**, 353.
42 C. Saint Flour and E. Papirer, *J. Colloid Interface Sci.*, 1983, **91**, 69.
43 J. B. Donnet, S. J. Park and H. Balard, *Chromatographia*, 1991, **31**, 434.
44 M. M. Chehimi and E. Pigois-Landureau, *J. Mater. Chem.*, 1994, **4**, 741.
45 T. Hamieh and J. Schultz, *J. Chim. Phys.*, 1996, **93**, 1292.
46 T. Hamieh, M. Rageul-Lescouet, M. Nardin and J. Schultz, *J. Chim. Phys.*, 1996, **93**, 1332.
47 E. Brendlé and E. Papirer, *J. Colloid Interface Sci.*, 1997, **194**, 207.
48 E. Brendlé and E. Papirer, *J. Colloid Interface Sci.*, 1997, **194**, 217.
49 F. M. Fowkes, *J. Adhes. Sci. Technol.*, 1990, **4**, 669.
50 J. C. Berg, in *Wettability*, ed. J. C. Berg, Marcel Dekker, New York, 1993, ch. 2.
51 J. C. Dobrowolski, M. H. Jamroz and A. P. Mazurek, *J. Mol. Struct.*, 1992, **275**, 203.
52 P. Jacob, D. Arola and J. C. Berg, *J. Appl. Polym. Sci.*, 1994, **51**, 695.
53 C. M. Bertelsen, MSc thesis dissertation, University of Cincinnati, 1997.
54 C. M. Bertelsen and F. J. Boerio, *J. Adhes.*, 1999, **70**, 259.
55 G. A. Woods, PhD Thesis dissertation, University of Liverpool, 1999.
56 M-L. Abel, A. Rattana and J. F. Watts, *J. Adhes.*, 2000, **73**, 313.